AFRL-RZ-WP-TP-2010-2082

MICROSTRUCTURAL CHARACTERIZATION OF $YBa_2Cu_3O_{7-x}$ FILMS WITH $BaZrO_3$ NANORODS GROWN ON VICINAL $SrTiO_3$ SUBSTRATES (POSTPRINT)

F. Javier Baca, Timothy J. Haugan, Joshua Reichart, and Paul N. Barnes

Mechanical Energy Conversion Branch
Power Division

Rose Lyn Emergo and Judy Z. Wu

University of Kansas

MARCH 2010

AIR FORCE RESEARCH LABORATORY
PROPULSION DIRECTORATE
WRIGHT-PATTERSON AIR FORCE BASE, OH 45433-7251
AIR FORCE MATERIEL COMMAND
UNITED STATES AIR FORCE

REPORT DOCUMENTATION PAGE

Form Approved
OMB No. 0704-0188

1. REPORT DATE *(DD-MM-YY)*	2. REPORT TYPE	3. DATES COVERED *(From - To)*
March 2010	Journal Article Postprint	01 July 2007 – 01 July 2009

4. TITLE AND SUBTITLE

MICROSTRUCTURAL CHARACTERIZATION OF $YBa_2Cu_3O_{7-x}$ FILMS WITH $BaZrO_3$ NANORODS GROWN ON VICINAL $SrTiO_3$ SUBSTRATES (POSTPRINT)

5a. CONTRACT NUMBER
In-house

5b. GRANT NUMBER

5c. PROGRAM ELEMENT NUMBER
62203F

6. AUTHOR(S)

F. Javier Baca, Timothy J. Haugan, Joshua Reichart, and Paul N. Barnes (AFRL/RZPG)
Rose Lyn Emergo and Judy Z. Wu (University of Kansas)

5d. PROJECT NUMBER
3145

5e. TASK NUMBER
32

5f. WORK UNIT NUMBER
314532ZE

7. PERFORMING ORGANIZATION NAME(S) AND ADDRESS(ES)

Mechanical Energy Conversion Branch (AFRL/RZPG)
Power Division
Air Force Research Laboratory, Propulsion Directorate
Wright-Patterson Air Force Base, OH 45433-7251
Air Force Materiel Command, United States Air Force

University of Kansas
Department of Physics and Astronomy
Lawrence, KS 66045

8. PERFORMING ORGANIZATION REPORT NUMBER
AFRL-RZ-WP-TP-2010-2082

9. SPONSORING/MONITORING AGENCY NAME(S) AND ADDRESS(ES)

Air Force Research Laboratory
Propulsion Directorate
Wright-Patterson Air Force Base, OH 45433-7251
Air Force Materiel Command
United States Air Force

10. SPONSORING/MONITORING AGENCY ACRONYM(S)
AFRL/RZPG

11. SPONSORING/MONITORING AGENCY REPORT NUMBER(S)
AFRL-RZ-WP-TP-2010-2082

12. DISTRIBUTION/AVAILABILITY STATEMENT

Approved for public release; distribution unlimited.

13. SUPPLEMENTARY NOTES

Journal article published in the *IEEE Transactions on Applied Superconductivity*, Vol. 19, No. 3, June 2009.
PA Case Number: 88ABW-2009-2978; Clearance Date: 01 Jul 2009.

14. ABSTRACT

When grown on miscut $SrTiO_3$ substrates, significant microstructural changes are observed in $BaZrO_3$-doped $YBa_2Cu_3O_{7-x}$ thin films when compared to those on non-vicinal substrates. Scanning Electron Microscopy indicates a surface morphology strongly influenced by the vicinal angle, and an accumulation of $BaZrO_3$ particles is observed near the step edges. Cross-sectional Transmission Electron Microscopy reveals that while the columnar formations of $BaZrO_3$ rods typically seen on non-vicinal substrates are present, a significant increase in planar defects in a 10 vicinal film are observed. The effects observed with increasing miscut angle indicate that the modulated surface provided by the vicinal substrate influences the crystalline quality of the YBCO matrix and BZO columnar formation through the thickness ofthe film.

15. SUBJECT TERMS

superconductivity, flux pinning, critical current density, magnetic field, $YBa_2Cu_3O_{7-x}$ or YBCO, $BaZrO_3$, nanorods, vicinal substrates

16. SECURITY CLASSIFICATION OF:			17. LIMITATION OF ABSTRACT:	18. NUMBER OF PAGES	19a. NAME OF RESPONSIBLE PERSON (Monitor)
a. REPORT	b. ABSTRACT	c. THIS PAGE			Timothy J. Haugan
Unclassified	Unclassified	Unclassified	SAR	10	19b. TELEPHONE NUMBER *(Include Area Code)* N/A

Standard Form 298 (Rev. 8-98)
Prescribed by ANSI Std. Z39-18

Microstructural Characterization of $YBa_2Cu_3O_{7-x}$ Films With $BaZrO_3$ Nanorods Grown on Vicinal $SrTiO_3$ Substrates

F. Javier Baca, Rose Lyn Emergo, Judy Z. Wu, Timothy J. Haugan, Joshua N. Reichart, and Paul N. Barnes

***Abstract*—When grown on miscut $SrTiO_3$ substrates, significant microstructural changes are observed in $BaZrO_3$-doped $YBa_2Cu_3O_{7-x}$ thin films when compared to those on non-vicinal substrates. Scanning Electron Microscopy indicates a surface morphology strongly influenced by the vicinal angle, and an accumulation of $BaZrO_3$ particles is observed near the step edges. Cross-sectional Transmission Electron Microscopy reveals that while the columnar formations of $BaZrO_3$ rods typically seen on non-vicinal substrates are present, a significant increase in planar defects in a 10° vicinal film are observed. The effects observed with increasing miscut angle indicate that the modulated surface provided by the vicinal substrate influences the crystalline quality of the YBCO matrix and BZO columnar formation through the thickness of the film.**

***Index Terms*—BZO, HTS, microstructure, vicinal substrate, YBCO.**

I. Introduction

THE growth of $YBa_2Cu_3O_{7-x}$ (YBCO) thin films has been extensively studied to improve their epitaxial quality on coated metallic substrates and single crystal ceramic substrates [1]–[4]. The resultant microstructural quality is important as it can affect the superconducting properties of the YBCO thin films, including the transition temperature (T_c) through lattice strain and the critical current density (J_c) with, for example, the presence of high angle grain boundaries [3]–[6]. Many of the growth parameters influence the epitaxial quality of a thin film, such as the mismatch between lattice parameters of the substrate and the deposited material, growth temperature, and the substrate surface qualities [7]–[11]. But other microstructural qualities, such as defect structures are also important as they play a significant role in vortex pinning and hence directly affect the J_c behavior in an applied magnetic field [12], [13].

Many methods have been explored to control the defect structures introduced into the YBCO matrix, with considerable success achieved in improving the flux-pinning properties by the addition of second-phase materials such as Y_2BaCuO_5, $BaSnO_3$, and $BaZrO_3$ [14]–[17]. Through the combination of substrate surface modification and second-phase material addition, finer control of structural properties can be achieved and has shown that superconducting properties are indeed improved [18], [19]. In this paper, we make a preliminary examination of the surface morphology and microstructural changes induced by depositing $BaZrO_3$ (BZO) doped YBCO on miscut $SrTiO_3$ (STO) substrates. While BZO has been well studied as a second-phase material for flux pinning, and has been shown to produce columnar defects aligned generally along the YBCO c-axis [17], we show some evidence of morphological and structural changes associated with the deposition of thin films of these materials on miscut STO substrates.

II. Experimental

Targets of YBCO with BZO concentrations of 2, 4, and 6 percent (by volume) were mixed, pressed and sintered from commercially available powders. STO substrates with miscut angles of 0° (non-vicinal), 5°, 10°, 15° and 20° were ultrasonically cleaned and mounted in the deposition chamber using colloidal Ag paint. YBCO + BZO films of 160–240 nm thickness were deposited by pulsed laser deposition (PLD) using a KrF excimer laser ($\lambda = 248\,\mathrm{nm}$) at a pulse rate of 8 Hz and energy density of $\sim 3.2\,\mathrm{J/cm^2}$. The films were grown at 810°C in an O_2 partial pressure of 300 mTorr, and the samples were cooled to 500°C in 1 atm O_2 and held at this temperature for 30 min.

Measurement of the transport current densities in the BZO doped YBCO films were made by four probe contact in self-field as well as with an applied magnetic field. T_c of the samples were obtained by resistive measurements. Magnetically inferred J_c as a function of applied magnetic field was also measured for the non-vicinal films using a Vibrating Sample Magnetometer (Quantum Design PPMS).

Surface morphology was examined using an FEI Sirion FEG high-resolution scanning electron microscope (SEM) at 5–15 kV. In order to observe the microstructural effects induced in the thin film by the inclined (001) plane of the miscut substrate, TEM cross-sections were cut from the samples along the direction transverse to the surface steps. To control the orientation of the cross-sections with respect to the vicinal terraces, focused

Manuscript received August 27, 2008. First published June 30, 2009; current version published July 15, 2009. This work was supported in part by the Air Force Research Laboratory and Office of Scientific Research. Corresponding author: F. J. Baca (e-mail: francisco.baca@wpafb.af.mil; jbaca@ku.edu).

F. J. Baca is with the Air Force Research Laboratory, WPAFB, OH 45433 USA, and also with the University of Kansas, Department of Physics and Astronomy, Lawrence, KS 66045 USA (e-mail: francisco.baca@wpafb.af.mil; jbaca@ku.edu).

R. L. Emergo and J. Z. Wu are with the University of Kansas, Department of Physics and Astronomy, Lawrence, KS 66045 USA (e-mail: remergo@ku.edu; jwu@ku.edu).

T. J. Haugan and P. N. Barnes are with the Air Force Research Laboratory, WPAFB, OH 45433 USA (e-mail: timothy.haugan@wpafb.af.mil; paul.barnes@wpafb.af.mil).

Digital Object Identifier 10.1109/TASC.2009.2017908

ion beam (FIB) systems (FEI Nova 600 NanoLab and DB235) were used for section cutting and lift out. Cross-sectional microstructure was studied using a Philips CM200 (LaB_6) TEM operating at 200 kV.

III. Results and Discussion

Detailed analyses of the transport J_c and resistive T_c measurements are shown elsewhere [20], however the T_c of the non-vicinal films was shown to decrease as the BZO concentration was increased from 2 vol.% to 6 vol.% and ranged from 89 K to 85 K. However, this decrease in T_c that is typically observed with the inclusion of second-phase defects has been shown to be less substantial for the vicinal films [20]. Magnetic J_c values for the non-vicinal films at 77 K and self-field ranged from 1.6 to 1.9 MA/cm^2 for BZO concentrations of 2, 4 and 6 vol.% and showed enhanced vortex pinning for applied magnetic fields greater than 1.2 T, 0.8 T, and 2.7 T, respectively (when compared to pure YBCO). Transport current measurements of the vicinal films showed increased J_c values for both self-field and in an applied magnetic field [20].

The surface morphology of the BZO-doped YBCO films, as observed by SEM, for BZO concentrations of 4 vol.% and 6 vol.% and vicinal angles of 0°, 5°, 10° and 20° are shown in Fig. 1. Significant changes in the YBCO surface properties are observable as the substrate miscut angle is increased. As the vicinal angle increases from 5° to 20°, terraces become increasingly pronounced, and typical terrace widths decrease from approximately 131 nm to 76 nm with respect to the substrate surface. Since the widths of the substrate terraces are expected to change proportionally with the cotangent of the miscut angle [9], the observed decrease indicates a consistent trend in the widths of the BZO-doped YBCO films.

At high magnification, contrast on particles of higher intensity can be seen on the film surface. As shown in Fig. 1, the largest and most densely arranged particles tend to form toward the vertices of the vicinal steps. It has been previously shown that YBCO grows via a step-flow mode on vicinal STO [8], and the anisotropic accumulation of second phase material on the surface terraces may be an indication that preferential formation at the step edges is similarly followed by BZO.

Table I summarizes the average sizes and densities of the surface particles as measured from SEM images at a higher magnification. It demonstrates that increasing the BZO content from 2 to 6 vol.% increases the particle density by a factor of approximately 1.8 on the non-vicinal substrates. However, the average size of individual (non-agglomerated) particles is slightly reduced (by a factor of ~1.4) when the BZO content is increased from 2 to 6 vol.%. The apparent discrepancy in the relative BZO surface area may be due to the lack of BZO nanorods extending completely through the thickness of the films and a greater fraction of the BZO occupying the subsurface volume as the vicinal angle increases. This conjecture is supported by cross-sectional imaging. The surface images also show that agglomeration and clustering of BZO nanoparticles into larger islands becomes more prominent in the vicinal films as the volume concentration is increased.

Although they are not visible in Fig. 1, a small number of rectangular outgrowths, likely indicative of a-axis oriented grains, are also observable at lower magnification of the surface of the non-vicinal 6 vol.% BZO sample. The appearance of a-axis oriented grains at 6 vol.% may indicate that the YBCO microstructural quality is affected by the increased dopant concentration in the non-vicinal films. However, it is notable that the vicinal films do not show such growths, which may indicate that the

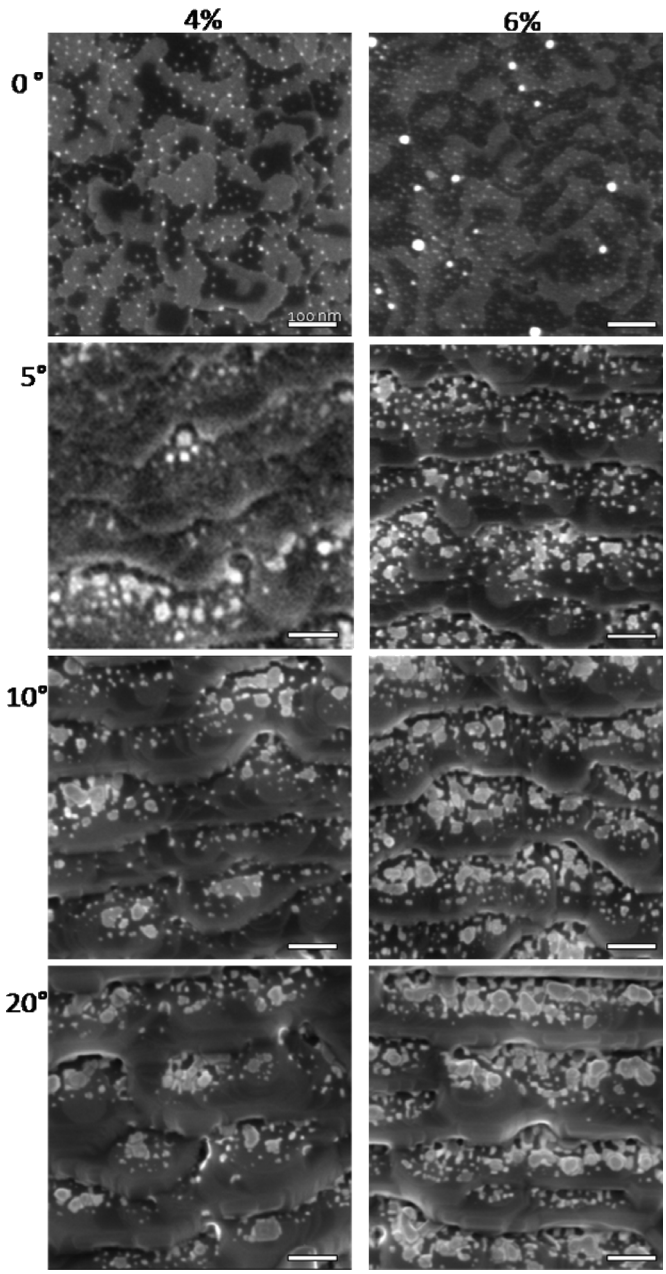

Fig. 1. SEM surface images of the YBCO + BZO (4 and 6 vol.%) samples on STO substrates with vicinal angles of 0°, 5°, 10°, and 20°. The scale bars indicate 100 nm.

TABLE I
BZO Surface Particle Area Density and Size

BZO Concentration (vol. %)	Avg. Surface Particle Size (nm)	Avg. Surface Particle Area Density (cm^{-2})
2	7.1 ± 1.2	1.21×10^{11}
4	6.6 ± 1.0	1.65×10^{11}
6	5.0 ± 0.9	2.13×10^{11}

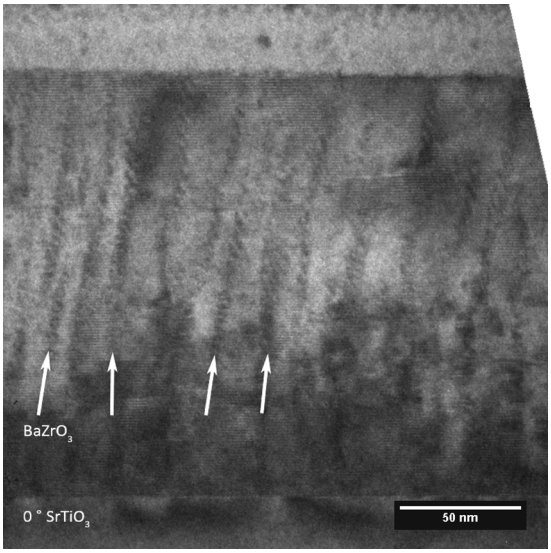

Fig. 2. Bright-field cross-sectional TEM image of a YBCO film doped with 2 vol.% BZO deposited on a non-vicinal (0°) STO substrate. The image confirms that columnar BZO rods (arrows) form on the non-vicinal films, and shows the relatively well-structured YBCO matrix.

modulated substrate surface provides a mechanism that allows for growth without the structural defects leading to these grain formations. Since a-axis oriented grains become more prominent as the YBCO film thickness is increased, this may suggest that the vicinal films may better accommodate the growth of thicker c-axis oriented films. Additionally, the surface morphologies shown in Fig. 1 clearly show variation with both the increased BZO content as well as with increased vicinal angle, and imply that microstructural changes are occurring. For this reason, cross-sectional TEM was utilized to further investigate the microstructural modification induced by the vicinal substrate.

Figs. 2 and 3 show initial TEM images that illustrate some of the effects of the vicinal substrates on the microstructure of the YBCO films containing 2 vol.% BZO. The bright-field cross-sectional TEM image in Fig. 2 confirms that the non-vicinal (0°) samples form BZO columns of approximately 5.2 nm in diameter that are aligned roughly along the YBCO c-axis. This type of columnar BZO formation has been widely observed in previous studies [17], [21], [22]. However, a significantly different microstructure is seen in Fig. 3(a), which shows a cross-sectional micrograph of a 2 vol.% BZO film grown on a 10° miscut STO substrate. In this image it is notable that the occurrence of planar defects, such as stacking faults, becomes abundant. It is also evident that the BZO forms in a columnar fashion, as on the non-vicinal substrates, and some of the planar defects can be seen to terminate at the column edges.

Fig. 3(b) shows a higher resolution image of a BZO column and the surrounding YBCO matrix. In this image, two regions of increased contrast that contain such planar defects are observable, and are separated by approximately 14 nm of relatively uniform material. The reduced intensity that provides contrast to these regions when compared to the surrounding material is likely to indicate increased structural strain, and the presence of dislocations at the YBCO/BZO interface are indeed visible.

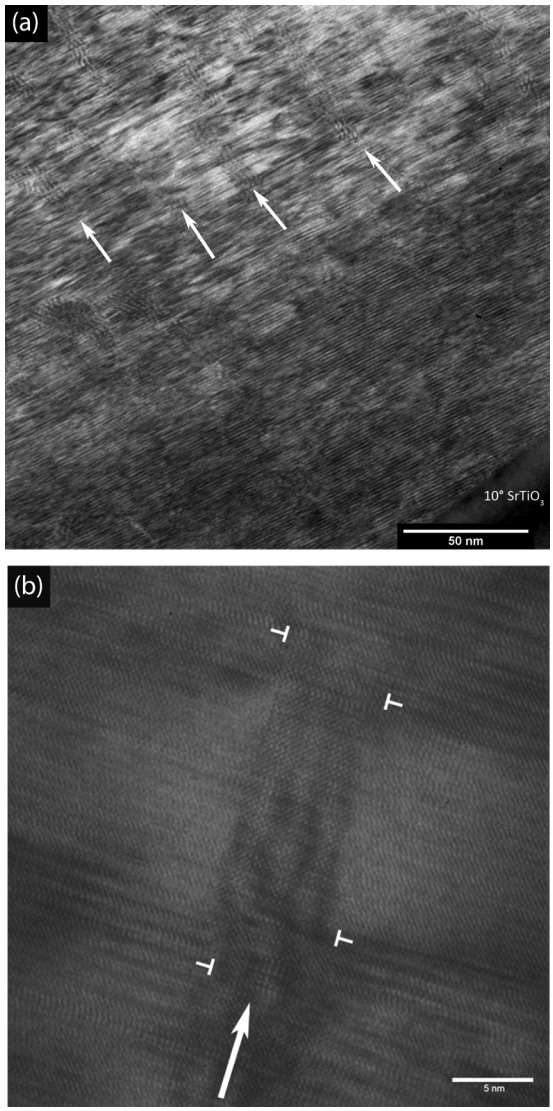

Fig. 3. Bright-field cross-sectional TEM images showing a YBCO film doped with 2 vol.% BZO grown on a 10° miscut STO substrate. (a) Lower magnification image showing abundant planar defects (50 nm scale bar). (b) Higher resolution micrograph with observed dislocations along the BZO column marked (5 nm scale bar). Arrows indicate examples of BZO nanorods.

Since the planar defects appear to coincide with the dislocations at the YBCO/BZO interface, this may provide evidence that the dislocations are inducing effects on the YBCO microstructure over longer distances than in the non-vicinal films, which do not display the prevalence of such planar defects. Since the miscut angle has been shown to affect the epitaxial quality (degree of c-axis orientation) of YBCO films [23], it should be expected that different miscut angles may further influence the microstructural properties of the BZO doped YBCO. For this reason, TEM studies on the other miscut angles and BZO concentrations are in progress.

IV. Conclusion

We have shown that BZO doped YBCO thin films deposited on miscut STO substrates undergo significant morphological and structural changes when compared to films deposited on

non-vicinal STO. Particles on the film surface are observed to preferentially form near the edges of vicinally-induced terraces. Since the surface energy is known to be higher at steps [8], these areas provide favorable nucleation sites for a deposited material. As the clustering of surface particles indicates, the BZO growth within the YBCO matrix also appears to favor these positions of higher surface energy.

Additionally, TEM cross-sectional images indicate that significantly more extended planar defects are observed in films deposited on 10° miscut substrates when compared to the same film on a non-vicinal substrate. Further examination indicates the presence of dislocations at the YBCO/BZO interface within the vicinity of the planar defects, which may imply that the extent of their structural effects is increased by the miscut substrate.

Since the surface morphology shows considerable variation with the increased substrate miscut angle and with BZO concentration, and since the miscut angle is known to influence the epitaxial quality [8], studies are in progress to investigate the effects of these parameters on the BZO formation and the effects on the YBCO microstructure and superconducting properties.

REFERENCES

[1] G. Kastner, D. Hesse, R. Scholz, H. Koch, F. Ludwig, M. Lorenz, and H. Kittel, "Microstructure defects in YBCO thin films," *Physica C*, vol. 243, pp. 281–293, 1995.

[2] A. Goyal, S. X. Ren, E. D. Specht, D. M. Kroeger, R. Feenstra, and D. Norton *et al.*, "Texture formation and grain boundary networks in rolling assisted biaxially textured substrates and in epitaxial YBCO films on such substrates," *Micron*, vol. 30, pp. 463–478, 1999.

[3] D. Larbalestier, A. Gurevich, D. M. Feldmann, and A. Polyanskii, "High- $\mathrm{T_c}$ superconducting materials for electric power applications," *Nature*, vol. 414, pp. 368–377, 2001.

[4] H. Wang, S. R. Foltyn, P. N. Arendt, Q. X. Jia, J. L. MacManus-Driscoll, and L. Stan *et al.*, "Microstructure of SrTiO3 buffer layers and its effects on superconducting properties of $\mathrm{YBa_2Cu_3O_{7-d}}$ coated conductors," *J. Mater. Res.*, vol. 19, pp. 1869–1875, 2004.

[5] A. Gurevich and E. A. Pashitskii, "Enhancement of superconductivity at structural defects in high-temperature superconductors," *Phys. Rev. B*, vol. 56, pp. 6213–6225, 1997.

[6] J. L. Reeves, D. M. Feldmann, C.-Y. Yang, and D. C. Larbalestier, "Current barriers in Y-Ba-Cu-0 coated conductors," *IEEE Trans. Appl. Supercond.*, vol. 11, pp. 3863–3867, 2001.

[7] J.-L. Maurice, J. Briatico, D.-G. Crete, J.-P. Contour, and O. Durand, "Effects of surface miscuts on the epitaxy of $\mathrm{YBa_2Cu_3O_{7-d}}$ and $\mathrm{NdBa_2Cu_3O_{7-g}}$ on $\mathrm{SrTiO_3}$ (001)," *Phys. Rev. B*, vol. 68, pp. 115429-1–115429-7, 2003.

[8] T. Haage, J. Zegenhagen, J. Q. Li, H.-U. Habermeier, M. Cardona, and C. Jooss *et al.*, "Transport properties and flux pinning by self-organization in $\mathrm{YBa_2Cu_3O_{7-d}}$ films on vicinal $\mathrm{SrTiO_3}$ (001)," *Phys. Rev. B*, vol. 56, pp. 8404–8418, 1997.

[9] L. Mechin, P. Berghuis, and J. E. Evetts, "Properties of YBa Cu O thin films grown on vicinal $\mathrm{SrTiO_3}$ (001) substrates," *Physica C*, vol. 302, pp. 102–112, 1998.

[10] F. J. Baca, D. Fisher, R. L. S. Emergo, and J. Z. Wu, "Pore formation and increased critical current density in $\mathrm{YBa_2Cu_3O_x}$ films deposited on a substrate surface modulated by $\mathrm{Y_2O_3}$ nanoparticles," *Supercond. Sci. Technol.*, vol. 20, pp. 554–558, 2007.

[11] Z. Chen, F. Kametani, S. I. Kim, D. C. Larbalestier, H. W. Jang, K. J. Choi, and C. B. Eom, "Influence of growth temperature on the vortex pinning properties of pulsed laser deposited $\mathrm{YBa_2Cu_3O_{7-x}}$ thin films," *J. Appl. Phys.*, vol. 103, pp. 043913-1–043913-7, 2008.

[12] G. Blatter, M. V. Feigel'man, V. B. Geshkenbein, A. I. Larkin, and V. M. Vinokur, "Vortices in high-temperature superconductors," *Rev. Mod. Phys.*, vol. 66, pp. 1125–1388, 1994.

[13] R. P. Huebener, *Magnetic Flux Structures in Superconductors*, 2nd ed. Berlin: Springer, 1979, pp. 179–194.

[14] T. Haugan, P. N. Barnes, R. Wheeler, F. Meisenkothen, and M. Sumption, "Addition of nanoparticle dispersions to enhance flux pinning of the $\mathrm{YBa_2Cu_3O_{7-x}}$ superconductor," *Nature*, vol. 430, pp. 867–870, 2004.

[15] C. V. Varanasi, P. N. Barnes, J. Burke, L. Brunke, I. Maartense, T. J. Haugan, E. A. Stinzianni, K. A. Dunn, and P. Haldar, "Flux pinning enhancement in $\mathrm{YBa_2Cu_3O_{7-x}}$ films with $\mathrm{BaSnO_3}$ nanoparticles," *Supercond. Sci. Technol.*, vol. 19, pp. L37–L41, 2006.

[16] J. L. MacManus-Driscoll, S. R. Foltyn, Q. X. Jia, H. Wang, A. Serquis, and L. Civale *et al.*, "Strongly enhanced current densities in superconducting coated conductors of $\mathrm{YBa_2Cu_3O_{7-x}} + \mathrm{BaZrO_3}$," *Nature Materials*, vol. 3, pp. 439–443, 2004.

[17] A. Goyal, S. Kang, K. J. Leonard, P. M. Martin, A. A. Gapud, and M. Varela *et al.*, "Irradiation-free, columnar defects comprised of self-assembled nanodots and nanorods resulting in strongly enhanced flux-pinning in $\mathrm{YBa_2Cu_3O_{7-\delta}}$ films," *Supercond. Sci. Technol.*, vol. 18, pp. 1533–1538, 2005.

[18] R. L. S. Emergo, J. Z. Wu, T. J. Haugan, and P. N. Barnes, "Tuning porosity of $\mathrm{YBa_2Cu_3O_{7-d}}$ vicinal films by insertion of $\mathrm{Y_2BaCuO_5}$ nanoparticles," *Appl. Phys. Lett.*, vol. 87, pp. 232503-1–232503-3, 2005.

[19] J. Z. Wu, R. L. S. Emergo, X. Wang, G. Xu, T. J. Haugan, and P. N. Barnes, "Strong nanopore pinning enhances J_c in $\mathrm{YBa_2Cu_3O_{7-d}}$ films," *Appl. Phys. Lett.*, vol. 93, pp. 062506-1–062506-3, 2008.

[20] R. L. Emergo, F. J. Baca, J. Z. Wu, T. J. Haugan, and P. N. Barnes, Combination of Nanopores and Nanorods Improves Overall $\mathrm{J_c(B,\theta)}$ in $\mathrm{YBa_2Cu_3O_{7-d}}$ Films, *to be published*.

[21] A. Ichinose1, K. Naoe, T. Horide, K. Matsumoto, R. Kita, M. Mukaida, Y. Yoshida, and S. Horii, "Microstructures and critical current densities of YBCO films containing structure-controlled $\mathrm{BaZrO_3}$ nanorods," *Supercond. Sci. Technol.*, vol. 20, pp. 1144–1150, 2007.

[22] S. Kang, A. Goyal, J. Li, P. Martin, A. Ijaduola, J. R. Thompson, and M. Paranthaman, "Flux-pinning characteristics as a function of density of columnar defects comprised of self-assembled nanodots and nanorods in epitaxial $\mathrm{YBa_2Cu_3O_{7-d}}$ films for coated conductor applications," *Physica C*, vol. 457, pp. 41–46, 2007.

[23] J. Kim, D. B. Chrisey, J. S. Horwitz, M. M. Miller, and C. M. Gilmore, "Growth mechanism of YBa2Cu3O7-d thin films and precipitates on planar and vicinal SrTiO3 substrates," *J. Mater. Res.*, vol. 15, pp. 596–613, 2000.